Submission code: G680BPWL6X

See this and other abstracts on our website: https://home.sbgf.org.br/Pages/resumos.php

Joint Inversion of Amplitude and Time-Shift Data for Improved Time-Shift Estimation

Ali Raeisdana (Heriot-Watt University), Colin MacBeth (Heriot-Watt University)

Joint Inversion of Amplitude and Time-Shift Data for Improved Time-Shift Estimation

Summary

This study examines a joint inversion method integrating amplitude and time-shift data to enhance time-shift estimation in seismic data analysis, addressing errors from wavelet interference, petro-elastic model (PEM) variability, and amplitude-kinematic coupling in conventional workflows. The approach incorporates PEM coefficients for geological consistency to refine velocity and impedance changes. Applied to 1D synthetic thin-reservoir model under water and gas injection scenarios, the method reduces mean absolute errors in time-shift estimation and velocity changes compared to traditional nonlinear inversion. Results demonstrate improved accuracy and physical consistency, particularly in complex, thin-layered reservoirs, advancing seismic interpretation by coupling amplitude and kinematic data while mitigating error propagation.

Introduction

The workflow for inverting time-shifts and amplitudes to velocity or impedance changes involves a well-known sequence of steps. First, time shifts between the baseline and monitor surveys are estimated. These time shifts are then applied to correct the monitor survey, aligning it with the baseline. Finally, 4D amplitudes are computed by subtracting the corrected monitor survey data from the baseline data. These time shifts and 4D seismic amplitudes may serve as attributes to interpret; however, commonly, time shifts are inverted further to time strain and velocity changes and 4D seismic amplitudes to changes in impedance (MacBeth et al., 2019). The accuracy of time-shift estimation is paramount in seismic inversion workflows, as it directly impacts the later stages of this workflow. Time-shift errors propagate through the inversion process, compromising the value of the interpretation (Duan et al., 2020). The primary sources of error include:

- *Wavelet interference*, which is exacerbated in thin layer reservoirs;
- *Variability in petro-elastic model (PEM) coupling*, which increases uncertainty in the inversion;
- *Amplitude-kinematic coupling,* which leads to correlated errors that hinder the separation of velocity and impedance changes.

These challenges are particularly acute in thin or stacked reservoirs with strong impedance contrasts, where amplitude-kinematic coupling serves to complicate the inversion process. Consequently, there is a need for methodologies that jointly invert amplitude and time-shift data to reduce such errors and improve the estimation and correlation between velocity and impedance changes. While most of the above challenges are well-documented in the context of 4D seismic inversion, finding a unified approach to address them collectively remains an ongoing challenge. Towards this objective, this study builds upon the iterative joint inversion methodology proposed by Zhan et al. (2017), introducing modifications to enhance its suitability for our problem. The original cost function introduced by Zhan is expressed as:

$$E = \|G * \Delta V/V - d'_{obs}\|_2^2 + \lambda\|\Delta V/V - (\Delta V/V)_0\|_2^2 \qquad (1)$$

Where *E* is the cost function, G is a linear forward operator, $\Delta V/V$ is time-lapse velocity changes, d'_{obs} is time-shift corrected 4D seismic amplitude, λ is the weight of regularization, and $(\Delta V/V)_0$ is the constraint to the initial low-frequency model. 4D seismic amplitudes are updated by converting inverted velocity changes to time shifts, and these updated amplitudes are subsequently used to iteratively refine the velocity change field. To achieve our primary outcome of this scheme to recover improved time shifts using the amplitude data that simultaneously satisfy both 4D amplitude changes and time-shifts, inspired by Williamson et al. (2007), we adapt this scheme to include a PEM coefficient. The methodology is applied to 1D synthetic data based on a thin reservoir for water and gas injection scenarios. (Figure 1 and Figure 3)

Method and/or Theory

The developed workflow includes a coefficient that accounts for PEM and follows the Zhan et al. (2017) workflow by substituting regularization terms with boundary to the initial model:

$$E = \|G * \alpha\, \Delta V/V - d'_{obs}\|_2^2 + \lambda_0 \|S_0 * \Delta V/V\| + \lambda_1 \|S_1 * \Delta V/V\| + \lambda_2 \|S_2 * \Delta V/V\|. \quad (2)$$

Where S_i is the i^{th} order Tikhonov regularization and λ_i is the regularization weight. Well-log calibrated PEM values (α) are incorporated to ensure geological consistency, it is possible to make distinctions between overburden and reservoir zones, enhancing the reliability of the inverted properties. Velocity changes derived from the inversion are converted iteratively into time shifts to update the 4D seismic amplitude (d'_{obs}). The results of this inversion workflow for water and gas injection scenarios are presented in Figures 2 and 4, showing the inverted velocity changes, recovered time-shifts, 4D seismic amplitude, and amplitude residual.

Results

This workflow is applied to a 1D synthetic baseline and monitor seismic data based on a thin reservoir geology. The results are analysed to assess the improvements in time-shift estimation and velocity changes. The recovered time-shifts are almost identical to the modelled time-shifts in both gas and water injection scenarios. Estimated time-shift results from the non-linear inversion method (NLI) (MacBeth et al., 2020) are also displayed in the figures for comparison purposes. This method significantly improves the time-shift estimation accuracy. The time-shift estimation mean absolute error value for the water injection scenario is 0.04% and for the gas injection scenario is 0.1%. The mean absolute error values for the inverted velocity changes are 0.18% and 0.28% for the water and gas scenarios, respectively. To prove that the proposed inversion workflow can catch the interferences, it is possible to close the loop by reconstructing the monitor data for each scenario and estimating NLI time-shift. Ideally, the estimated NLI time-shift between the observed monitor and reconstructed monitor should match perfectly. The observed monitor and reconstructed monitor, as well as the estimated time-shift between baseline and either of these monitors has been displayed. The mean absolute error between the originally estimated NLI and the secondary estimated NLI is 0.003%. Overall, our joint inversion workflows improved time-shift estimates compared to the initial NLI estimates, providing better physical consistency and closing the loop between modelling and inversion, which indicates that the proposed inversion scheme can cope with interferences. These results demonstrate the importance of joint inversion in thin reservoir analysis, where integrating both time-shift and amplitude data is crucial for reliable and accurate seismic interpretation.

Conclusions

This study has investigated the potential of joint inversion workflows for amplitude and time-shift data in seismic analysis, with a focus on overcoming challenges in time-shift estimation. By adopting an iterative approach, a method to enhance the resolution of seismic inversion outputs was demonstrated while addressing critical errors inherent in conventional workflows. The iterative joint inversion framework addresses the coupling of amplitude and time-shift data. This method exhibited a marginal advantage in time-shift accuracy, aligning with the study's objective of mitigating spurious estimates. In contrast to the conventional workflow—where velocity and impedance changes are decoupled, resulting in substantial errors—the proposed method forces a relationship between these parameters (α). The validation process, which utilised closing the loop between modelling and inversion, further reinforced the reliability of the proposed workflow. The integration of PEM ensured geological consistency, reinforcing the physical validity of the inversion results. The refined time-shift estimates, which more closely align with observed amplitude data, represent a significant advancement, improving the accuracy of seismic interpretation and enabling better applications in complex geological environments, such as thin reservoirs and high-contrast subsurface layers.

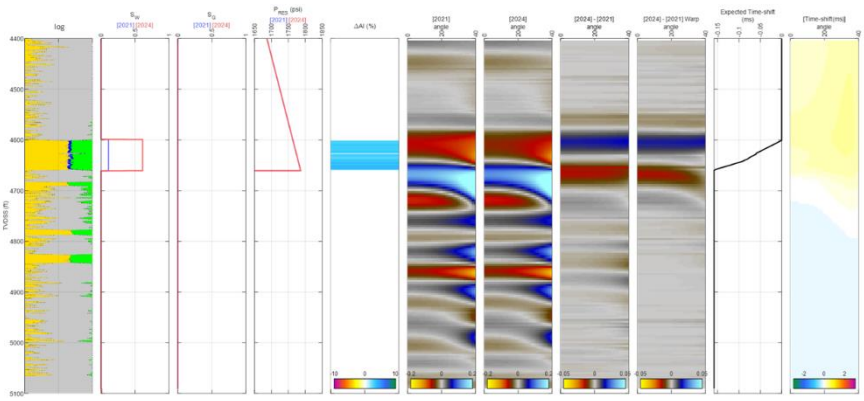

Figure 1. Water injection scenario. From left to right: log data; water saturation for the baseline and monitor; gas saturation for the baseline and monitor; pressure for the baseline and monitor; calculated impedance changes; synthetic seismic data for the baseline and monitor at angles ranging from 0° to 40°; raw 4D seismic amplitude; NLI time-shift corrected 4D seismic amplitude; true modelled time shift; and estimated NLI time shift in angles ranging from 0° to 40°.

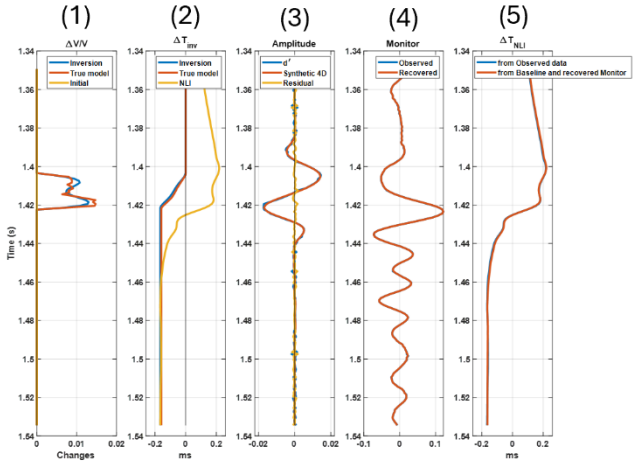

Figure 2. From left to right: (1) Velocity changes, where the true model is represented in red, inversion results in blue, and the zero initial model in yellow; (2) Time shift, with the true model in red, inversion results in blue, and NLI estimations in yellow; (3) 4D amplitude, where d'_{obs} for the final iteration is shown in blue, the synthetic 4D amplitude in red, and the amplitude residual in yellow; (4) Monitor seismic data, where the observed monitor is in blue and the recovered monitor in red; (5) NLI time shifts, with the estimated NLI from the baseline and monitor shown in blue, and the estimated NLI from the baseline and recovered monitor in red.

Acknowledgments

This research was supported by the sponsors of the ETLP Phase VIII and Phase IX projects. Their contributions are gratefully acknowledged. (https://etlp.hw.ac.uk/sponsorship/) The authors also extend sincere appreciation to Sean Tian for his assistance and for providing access to the log2seis package, which was instrumental in this study.

References

Duan, Y., Yuan, S., Hatchell, P., Vila, J., & Wang, K. [2020] Estimation of time-lapse time shifts using machine learning. SEG Technical Program Expanded Abstracts 2020 (pp. 3724-3728).
Griffiths, L., Blanchard, T. D., Edgar, J. A., & Shahraeeni, M. S. [2015] Trace warping vs. impedance warping in 4D seismic inversion. 77th EAGE Conference and Exhibition

MacBeth, C., Amini, H., & Izadian, S. [2020]. Methods of measurement for 4D seismic post-stack time shifts. *Geophysical Prospecting*, *68*(9), 2637-2664.

MacBeth, C., Mangriotis, M., and Amini, H., [2019] Post-stack 4D seismic time-shifts: interpretation and evaluation. Geophysical Prospecting 67.1: 3-31

Rosa, D. R., Santos, J. M., Souza, R. M., Grana, D., Schiozer, D. J., Davolio, A., & Wang, Y. [2020] Comparing different approaches of time-lapse seismic inversion. Journal of geophysics and engineering, 17(6), 929-939.

Williamson, P.R., Cherrett, A.J. and Sexton, P.A. [2007] A new approach to warping for quantitative time-lapse characterisation. 69th EAGE Annual Meeting, London, Expanded Abstracts, P056.

Zhan, X., Chu, D., Wheelock, B., Johnston, D., Bandyopadhyay, K., & McAdow, D. [2017] 4D time shift and amplitude versus offset joint (AVO) inversion. In SEG International Exposition and Annual Meeting.

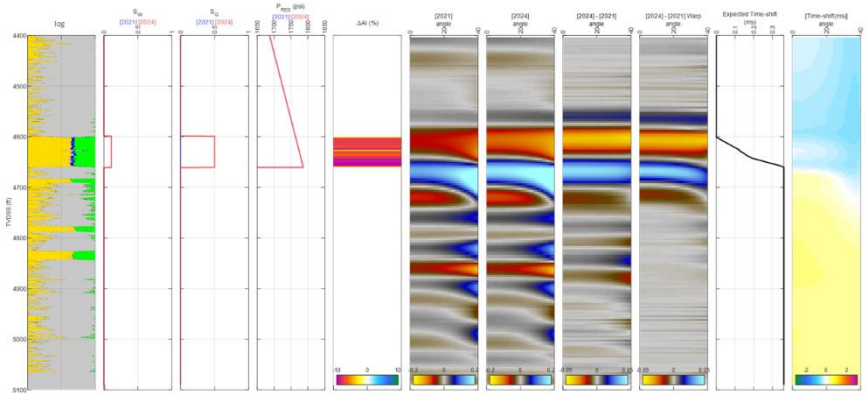

Figure 3. Gas injection scenario. From left to right: log data; water saturation for the baseline and monitor; gas saturation for the baseline and monitor; pressure for the baseline and monitor; calculated impedance changes; synthetic seismic data for the baseline and monitor at angles ranging from 0° to 40°; raw 4D seismic amplitude; NLI time-shift corrected 4D seismic amplitude; true modelled time shift; and estimated NLI time shift in angles ranging from 0° to 40°.

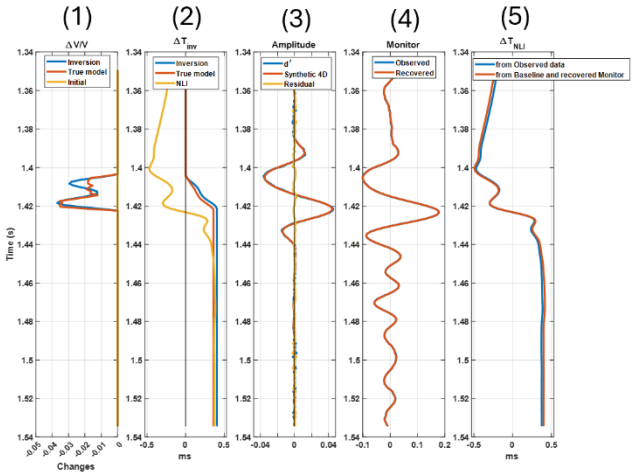

Figure 4. From left to right: (1) Velocity changes, where the true model is represented in red, inversion results in blue, and the zero initial model in yellow; (2) Time shift, with the true model in red, inversion results in blue, and NLI estimations in yellow; (3) 4D amplitude, where d'_{obs} for the final iteration is shown in blue, the synthetic 4D amplitude in red, and the amplitude residual in yellow; (4) Monitor seismic data, where the observed monitor is in blue and the recovered monitor in red; (5) NLI time shifts, with the estimated NLI from the baseline and monitor shown in blue, and the estimated NLI from the baseline and recovered monitor in red.